

# MODERN FLUID POWER

CHALLENGES · RESPONSIBILITIES · MARKETS

24th - 26th MARCH 2014 | PROCEEDINGS

9TH INTERNATIONAL FLUID POWER CONFERENCE



## GENERAL

Dirk Schulze Schencking

+49 (0) 241 - 80 27519  
general@ifk2014.de

## REFERENTS / PAPER

Katharina Schrank

+49 (0) 241 - 80 27522  
papers@ifk2014.de

## TRADE EXHIBITION

Jutta Zacharias

+49 (0) 241 - 80 20202  
exhibition@ifk2014.de

## ADDRESS

Steinbachstraße 53B  
D-52074 Aachen

+49 (0) 241 - 80 22194  
post@ifk2014.de  
www.ifas.rwth-aachen.de

9TH IFK | CONFERENCE PROCEEDINGS





# Hybrid Pump Model for 1D Hydraulic System Simulation

Heiko Baum \*, Klaus Becker\*\* and, Axel Faßbender \*\*

FLUIDON Gesellschaft für Fluidtechnik mbH, Jülicher Straße 338a, 52070 Aachen, Germany\*  
 Cologne University of Applied Sciences, Faculty of Automotive Systems and Production Engineering,  
 Betzdorfer Straße 2, 50679 Köln, Germany \*\*  
 E-Mail: heiko.baum@fluidon.com

This paper presents a novel approach to implement the dynamic displacement characteristic of a real pump into the 1D system simulation. In order to achieve this, the pump is measured under defined boundary conditions and these measurements then are used together with suitably adapted, classical physical modelling approaches to form a hybrid pump model.

Central part of the hybrid pump model are measurement data of two different test rig constellations. At the first test rig the pump's characteristic pressure pulsations are measured against a line termination without reflection (RaLa). At the second test rig the pump impedance is measured by means of the 2p/2s-approach.

In the hybrid pump model the pump's characteristic flow is represented by look-up tables calculated from the RaLa measurements and the impedance is represented by a  $\lambda/4$  resonance tube.

An automotive power steering pump is used to present the methodical work steps towards the construction of the hybrid pump model. The simulation of a ramp run-up of the pump will be compared towards the measurements. With this final simulation it is demonstrated that the hybrid pump model represents a suitable modelling approach to include the dynamic behaviour of a hydraulic displacement pump into the time domain based simulation.

The works underlying this paper have been carried out in the context of the ZIM project "OptiELF" sponsored by the German Federal Ministry of Economy and Technology in cooperation between Cologne University of Applied Sciences and FLUIDON GmbH.

**Keywords:** Impedance measurement, flow pulsation, pump simulation, pump test rig, measurement service

**Target audience:** Hydraulic pump manufacturer, mobile hydraulics, automotive industry

## 1 Introduction

At the background of a growing electrification of working machinery, traditional hydraulic systems are faced with new challenges. Among others the acoustic optimization of the systems in this context occupies an important position in further development activities. Positive displacement pumps are usually the main source of noise in hydraulic systems. This is predominantly a result of the flow ripple generated by the pumping mechanism. Due to the fluid-borne noise ability to spread in the external system, these flow pulsations are essential when evaluating pressure oscillation phenomena or the noise creation in a hydraulic system.

At the appearance of unwanted pressure oscillation phenomena, it is therefore necessary to include all system components in the problem analysis and to examine the oscillation behaviour or the resonance conditions for different system operation points. In order to achieve this, a pump run-up simulation, at which the system is excited by the pressure dependent and the speed dependent flow pulsation of the pump, would be best suitable.

While pipes, hoses and valves quite simply can be included into a time domain based simulation, the modelling of a pump, which is suitable for the analysis of the pressure oscillation behaviour of a hydraulic system, is still very effortful today. Usually a detailed physical pump model is required, to represent the pump's dynamic effects, such as the pump's flow pulsations or the pump impedance.

However, the design of such pump models requires constructive detail knowledge and is, due to the still necessary validation measurements and simulation, very costly and time consuming. Moreover, for a simulative analysis of pressure oscillation phenomena the mathematical pump models are only very restrictedly usable due to the long computing times even if they are available.

This paper introduces an alternative, measurement based modelling approach for a hydraulic pump for the 1D system simulation, at which an automotive vane pump will be measured, using already available and proven test methods. Afterwards, those measurements, together with suitably adapted, classical modelling techniques, will be combined to the hybrid pump model.

## 2 Pump Model Synthesis

One of the goals of the OptiELF project is the development of a measurement-based pump model that provides realistic flow pulsations to a 1D-system simulation's hydraulic circuit [1]. Application focus is the analysis of pressure ripple implied resonance phenomena in a complex hydraulic ducting. The model should be quickly parameterised through an automated measurement procedure and there should be no need for often confidential manufacturer information about the pumps internal design.

### 2.1 Theoretical Background

In the literature about the simulation of hydraulic pumps various attempts can be found for the model's setup. Some of them use a physically exact description [2] [3] [4], others use empirical substitute models [5] [6] [7].

In view of the complexity and the difference of the excitation mechanisms in a hydraulic pump, the use of a relatively simple pump model is recommendable. However, at the same time, it is desirable that this pump model must be applicable for all sorts of hydrostatic pumps, whereas the model parameters that have to be determined or to be measured are dependent on the pump alone and will not be influenced by the combination of pump and load system [6].

Many researchers, especially if the model is designed for a simulation in the frequency domain, refer to the standard 'Norton' model [6] [7] or an appropriate modification of this model [5] [8] [9] to describe the pump. Figure 1 gives a brief overview of commonly used representations for the 'Norton' model.

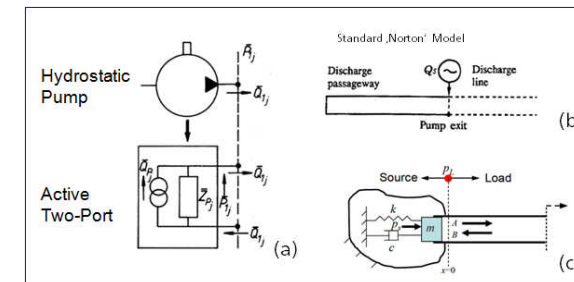


Figure 1: Pump representation as active dual pole and equivalent analogies (a) Stulemeijer [6], (b) Kojima[5], and (c) Liu[10]

The 'Norton' model (b) is the simplest representation of an active two-port (a), at which the pump's discharge passageway is modelled as a pipe. The model can be "tuned" to a specific frequency, usually the measured pump impedance, but a known disadvantage of this analogy is, that it will give poor results at higher frequencies. An approach to overcome this disadvantage is, to describe the pump's discharge passageway as a first order

oscillator (c) such as a hydraulic Helmholtz resonator or as a spring-mass-damper system. However, the parameter values for these first order models have to be "tuned" as well, and therefore do not resemble real physical parameters of the pump.

### 2.2 Pump Model Concept

The OptiELF pump model is only intended to represent the characteristic dynamical behaviour of a real pump in a system simulation model and shall not describe the pump in detail. Due to its simplicity, the 'Norton' model will be the basis modelling approach. To overcome its limitations the model will be extended by aspects of a wave decomposition approach, such as were presented by Liu and Herrin [10]. Figure 2 gives a schematic illustration of the wave decomposition premise.

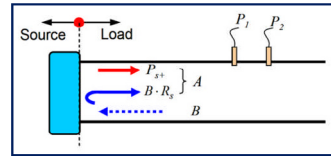


Figure 2: Schematic illustration of the wave decomposition premise [10]

According to the wave decomposition methodology the pump flange pressure  $p_L$  represents a superposition of the pump's outgoing pressure wave  $A$  and the system's reflection wave  $B$ . The outgoing pressure wave  $A$  is in the same manner a superposition of the pump's internal pressure  $p_{S^*}$  and the reflection of wave  $B$  at the pump's inner boundary, which can be expressed as  $B \cdot R_S$ .  $R_S$  represents the reflection factor of the pump. Equation (1) summarises these interrelations.

$$p_L = p_{S^*} + B \cdot (1 + R_S) \quad (1)$$

From Equation (1) it is obvious that in case of a reflection free measurement (RaLa), when the reflection wave  $B$  is zero, the pressure pulsation  $p_L$  at the pump flange is equal to the outgoing source pressure pulsation  $p_{S^*}$  of the pump. Because the pressure  $p_{S^*}$  already includes all influences of the pump's discharge passageway, the discharge passageway pipe of the intended 'Norton' equivalent model must not influence the shape of the pressure pulsation. Hence, it must have the same load impedance and as consequence of that the same diameter than the pipe that was used during the RaLa measurements. The discharge passageway pipe itself then can be treated like a  $\lambda/4$  resonator, and the pipe's length  $l_{RP}$  needs only be tuned by means of Equation (2) to match the frequency of the measured pump's impedance anti-resonance  $f_i$ .

$$l_{RP} = \frac{c_0}{4 \cdot f_i} \quad (2)$$

What is still missing in the pump model is its dynamic feedback  $B \cdot R_S$  of the discharge passageway pipe onto the pressure ripples  $B$  coming out of the load system. A suitable way to include the reflection into a simulation model is, to include a resistance into the resonance pipe. As part (1) of Figure 3 presents, in a time domain based simulation a reflection can easily be modelled, by placing an orifice type resistance between two pipes.

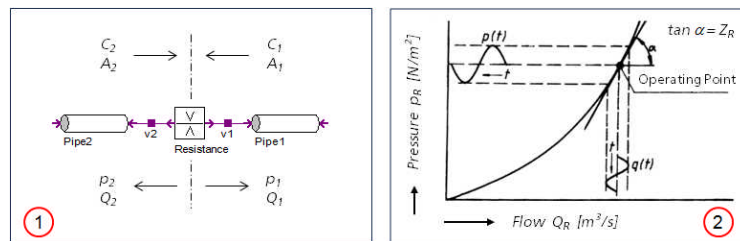


Figure 3: Resonance tube with orifice type resistance

(1) Example of a distributed parameter model; (2) Impedance of the orifice's operating point [6]

Part (2) of Figure 3 illustrates how the impedance of such an orifice can be expressed. It's the linearization of the characteristic pressure-flow-curve of the orifice at the present operating point ( $p_R$  and  $Q_R$ ). Equation (3) expresses the resulting impedance  $Z_R$  of the orifice.

$$Z_R = \frac{p_R}{Q_R} \quad (3)$$

Since the pressure-flow-curve of the orifice does have a non-linear characteristic, the orifice impedance  $Z_R$  needs to be recalculated for each operation point. During the simulation this is automatically done via an iteration that calculates the flow through the orifice, according to Equation (4).

$$Q_R = \frac{C_2 Z_2 - C_1 Z_1}{Z_R + Z_2 + Z_1} \quad (4)$$

In this equation  $C_1$  and  $C_2$  represent the wave characteristics of the connected pipes, which are programmed according to the method of characteristic, and  $Z_1$  and  $Z_2$  are the impedances of those pipes. Further information about the usage of the method of characteristics to model pipes for a time domain system simulation can be found at Habr [11] and at Müller [12].

The pressure  $p_1$ , which is one part of the reflection  $B \cdot R_S$ , is now calculated by means of Equation (5).

$$p_1 = (-Q_R - C_1) \cdot Z_1 \quad (5)$$

Because the origin of the flow ripple that leads to  $p_{S^*}$  can be assumed to be a high-impedance source, it is independent of the pressure and can be placed in parallel to the reflection calculation. With this assumption, Equation (5) can be rewritten as Equation (6).

$$p_1 = (Q_{S^*} - Q_R - C_1) \cdot Z_1 \quad (6)$$

The other part of the reflection  $B \cdot R_S$  is the flow  $Q_1$  that is calculated according to Equation (7).

$$Q_1 = Q_{S^*} - Q_R - \left( C_1 + \frac{p_1}{Z_1} \right) \quad (7)$$

Through an automated change of the pressure-flow-characteristic of the orifice, it is now possible to tune the reflection of the discharge passageway pipe so that the simulated pump impedance fits the measured impedance.

## 3 Measurements

In order to obtain the measurement data that are required for the setup of the hybrid pump model two different test rig constellations are necessary. The first test rig measures the pump's characteristic pressure pulsations against a reflection less line termination (RaLa). The second test rig measures the pump impedance by means of the 2p/2s-approach.

### 3.1 RaLa-Measurements

The RaLa test rig design is according to the setup introduced by Theissen [13], which was later also used by Rothmund [14]. In order to measure the flow pulsation, a straight pipe is connected to the pump, which at the other end is connected to a combination of orifice and volume. The orifice and volume combination is adjusted in a manner that forms a line termination without reflection of the passing pressure waves. Behind the RaLa a pressure relieve valve (PRV) is installed to adjust the static measurement pressure. A sketch of the test rig setup, together with a picture of the test rig, is presented in Figure 4. At both ends of the pipe are dynamic pressure sensors. In the reflection-free situation  $p_i$  is equivalent with  $p_{S^*}$ .

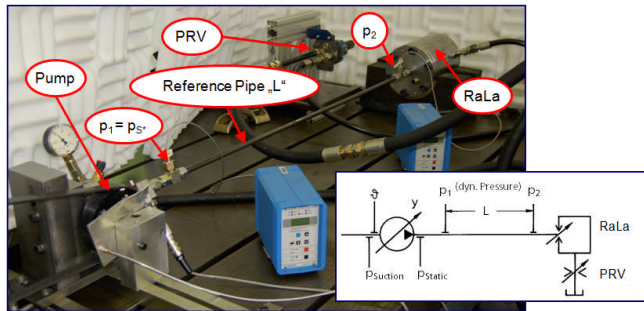


Figure 4: Set-up of the RaLa test rig

A detailed description how the dynamic pressure signals are analysed and how the variable orifice of the RaLa has to be tuned in order to achieve a measuring condition without reflection is described by Schellinger [15]. For the setup of the hybrid pump model, RaLa measurements at system pressures of 45, 50, and 55 bar as well as at pump speeds from 800 1/min to 3000 1/min in 50 1/min steps have been conducted. All of these 132 measurements are triggered according to the pump's angular position, so that each data set starts at the same rotor position. The measurements contain the pump's characteristic pressure pulsation for a rotation of 360°. Each pressure pulsation measurement  $p_{S^*}$  is transformed into a flow pulsation  $Q_{S^*}$  according to Equation (8).

$$Q_{S^*} = \frac{A_{RP}}{\rho \cdot c_0} \cdot p_{S^*} \quad (8)$$

The software tool "Pump Measurement Analyser", shown in Figure 5, has been developed for this task. Dependent on the number of chosen spectral lines out of the FFT spectrum of the pressure pulsation, it is possible to tune the frequency resolution of the resulting flow pulsation. Each calculated flow pulsation table is stored as x/y look-up table. The x-axis of the look-up table consists of angular position values between 0° and 360°. The y-axis is the pump flow.

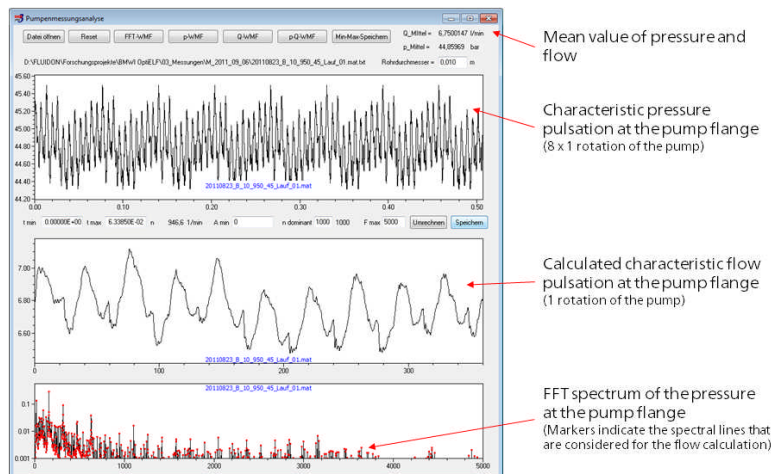


Figure 5: Conversion of the pressure pulsation into a flow pulsation

Figure 6 gives a first overview of the generated flow pulsation tables. Represented is the average pump flow in l/min versus the number of points in the look-up table. It is obvious that with an increasing pump speed the average pump flow increases but the number of data samples in the flow table declines.

The reason for this is the used constant sampling rate of the measurement system. At lower pump speeds there are more data samples per pump rotation in a measurement as it is the case for a higher pump speed. Because the time scale of the pump pulsation measurement is reused at the pump flow calculation (inverse FFT of the result

of Equation (8)), the effect of unequal data set lengths is consequently visible in the calculated flow pulsations as well.

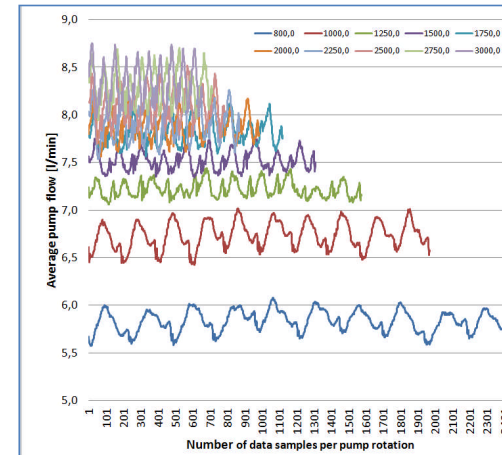


Figure 6: Flow pulsation characteristic of a 10-chamber vane pump at different pump speeds

The typical representation of data in a more dimensional look-up table is grid based on Cartesian coordinates. The unequal data set length of the calculated flow pulsation tables is disadvantageous for the later usage in such a regular look-up table. For the hybrid pump model therefore an alternative line-based look-up table representation has been developed (Figure 7). In order to generate the 2D-look-up table that is represented in Figure 7 the required second axis is defined as an array of 1D-look-up tables. Here these are the 44 pump speed operating points from 800 1/min to 3000 1/min. The optional third axis to describe a 3D-look-up table is defined as array of 2D-look-up tables. Here these are the three static pressure levels 45, 50, and 55 bar.

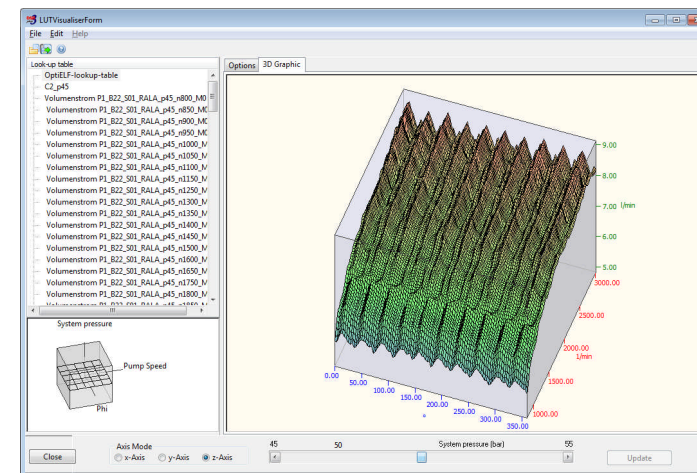


Figure 7: Final lookup-table of the pump's characteristic flow at different pump speeds

Besides its usage for the hybrid pump model, the flow pulsation look-up table can also be used to analyse the flow characteristics of the measured pump. Clearly visible for example, is the change in the characteristic flow pulsation for each of the 10 pump chambers versus the pump speed. Interesting is the distinct change of the flow fluctuation at around 1200 1/min when the pump's flow-control valve gets active. Moreover, the peak-to-peak variation of the flow pulsation versus the pump speed provides information about the absolute value of the flow fluctuation.

### 3.2 2p/2s-Measurements

The 2p/2s-test rig design (Figure 8) is according to the setup introduced by Kojima [5]. Together with other impedance measuring methods the 2p/2s-method has been evaluated by Berger [16] and was finally chosen as measurement method for the research work of the OptiELF project.

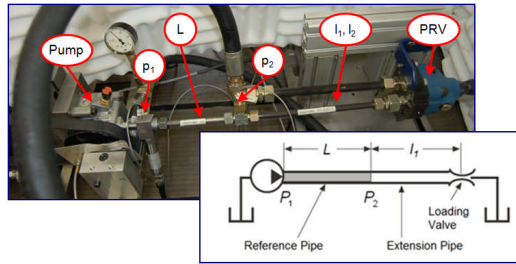


Figure 8: Set-up of the 2p/2s test rig

The 2p/2s-method can evaluate the source flow ripple and source impedance of the pump only by measuring the wave propagation characteristics of pressure ripple in the reference pipe alone, which is just a part of the discharge line adjustment to the pump exit [5]. With two measurements with different extension pipe lengths  $I_1$  and  $I_2$ , the pump impedance is according to Equation (9).

$$Z_S = jZ_c \frac{(P_1 - P'_1)\sin(\beta L)}{P_2 - P'_2 - (P_1 - P'_1)\cos(\beta L)} \quad (9)$$

The calculated pump impedance will be used to determine the length of the  $\lambda/4$  resonance pipe of the hybrid pump model and to verify the final hybrid pump model parameterization, through a comparison with the pump impedance calculated out of the simulation results.

### 4 Setup of the Hybrid Pump Model

The hybrid pump model has been modelled in a time domain based 1D system simulation program [17]. The mathematical description of the component models is according to the two-pole methodology, as it is explained for example by Stulemeijer [6]. Examples for the implementation of such component models into time domain based simulations are described by Müller [12]. Figure 9 shows the pump model. The pump symbol (1) is representing the flow source and uses the flow pulsation look-up table. Model input is the pump speed that is used to calculate the pump's rotating angle between  $0^\circ$  and  $360^\circ$  and to select between the 44 measurements of the pump speed operating points. The system pressure, as third input to the flow pulsation look-up table, is available through the connection to the rest of the simulation model.

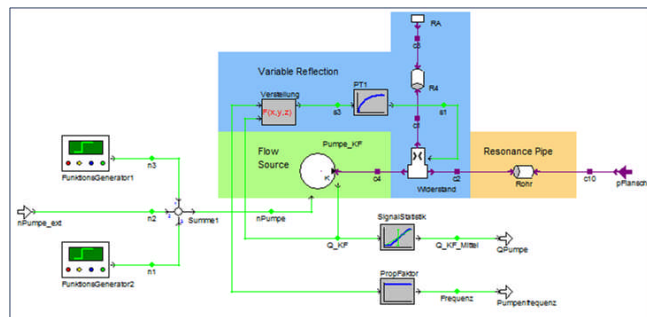


Figure 9: Simulation model representation of the pump

Directly behind the pump is the replacement model of the variable pump reflection (2). The opening of the orifice in the branching component can be adjusted by means of an equation block element. Thus, the impedance

of the orifice and consequently the reflection coefficient of the source can be tuned in dependence of the pump speed and the pump flow. The final part of the hybrid pump model is the  $\lambda/4$  resonance pipe (3) that does have the same diameter as the reference pipe of the RaLa measurement. For its later use in the system simulation, the entire model is encapsulated as a sub model.

### 5 Validation of the Hybrid Pump Model

The validation of the hybrid pump model will be undertaken in two steps. In a first test the model is used to conduct RaLa simulations. The second test is a run-up simulation of the pump under load. From this simulation the pump impedance is calculated and will be compared against the measured pump impedance.

#### 5.1 Simulation of RaLa Measurements

Figure 10 shows the simulation model of the RaLa test rig. The label "RaLa Measurement" marks a component that feeds the measured pressure pulsation into the simulation model. The label "Hybrid Pump Model" indicates the sub model of the pump.

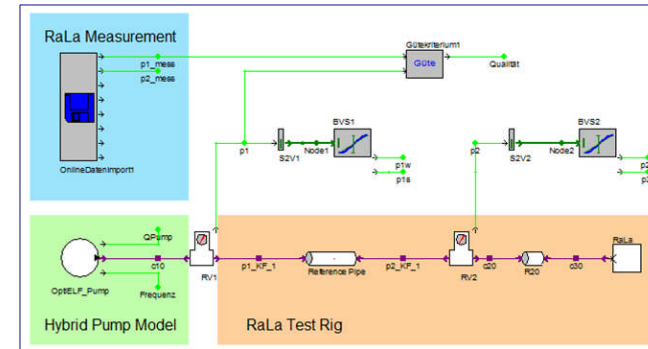


Figure 10: Simulation of the RaLa test rig

In order to judge the quality of the simulation, Figure 11 presents a comparison of measured and simulated pressure pulsations at different pump speeds. At this point it has to be mentioned that the presented measurements are not those measurements, which previously were used to calculate the flow pulsation look-up tables. This has been done on purpose to test the robustness of the modelling procedure.

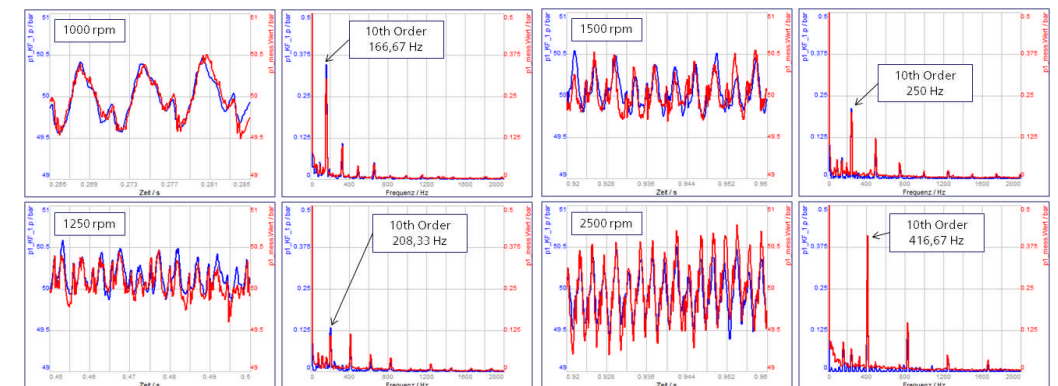


Figure 11: RaLa measurements and simulations at different pump speeds (red: measurement, blue: simulation)

For each of the graphics in *Figure 11*, there are time-based pressure values shown on the left hand side and the corresponding FFT spectra of this data are shown on the right hand side. For each comparison the data set length is 1 s so that for the 1000 rpm point there are at least 16 pump revolutions evaluated.

At the first represented pump speed (1000 1/min) the pump's flow controller is not yet active and the results show the pure geometric flow pulsation of the pump. The next two pump speeds cover the operating range of the pump, at which the flow controller becomes active. In both, time as well as frequency domain, it can be clearly seen that the pressure fluctuation declines during this period. The relation between 10th and 20th pump order becomes smaller as well. At a higher pump speed the pressure fluctuation is again dominated by the 10th pump order. Summing up, it can be stated that the hybrid pump model seems to be suitable to represent the pump's characteristic flow pulsation under quasi static load conditions.

### 5.2 Simulation of 2p/2s Test Rig Setup

The final test of the hybrid pump model is the comparison between measured and simulated pump impedances. A simulation model (*Figure 12*) has been modelled for this purpose that is identical to the 2p/2s test rig used for the measurements.

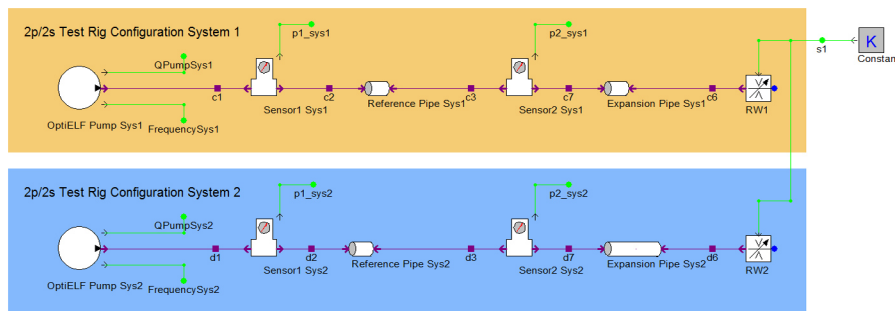


Figure 12: Simulation model of the 2p/2s-test rig

The upper part of the simulation model represents the test rig setup with short pipe lengths  $l_1$ , the lower part the setup with long pipe lengths  $l_2$ . Thus, both necessary data sets to calculate the pump impedance can be generated in only one simulation run. Identical to the measurement, the simulation's pump speed rises from 800 1/min up to 3000 1/min in about 48 s. In a subsequent order analysis the first five dominant pump orders are extracted from the measurement and from the simulation data set. *Figure 13* shows a comparison of the time domain and frequency domain results of this post processing.

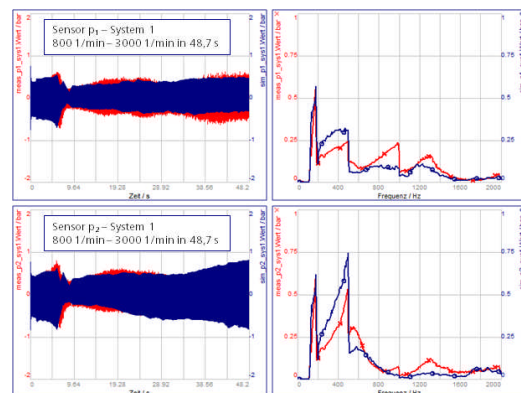


Figure 13: Comparison of the first 5 pump orders of a measured and a simulated pump run-up (red: measurement, blue: simulation)

The left two graphs show the dynamic pressure of  $p_1$  and  $p_2$  in test rig configuration 1. In both graphics the moment can be identified when the flow controller of the pump gets active after about 9 s. The dynamic pressure fluctuation suddenly decreases.

The right two graphs of *Figure 13* show the FFT spectra, calculated from the time domain values. The FFT spectra show a reasonable good correlation of the amplitudes up to 2000 Hz which is equal to an excitation of the system by the 40th pump order. Thus, it can be assumed that a simulation model equipped with the hybrid pump model will be stimulated with flow pulsations, which in amplitude and in frequency are very similar to those of the real pump.

The two data sets are then used to calculate the pump impedance according to Equation (9). The resulting impedances are shown in *Figure 14*. The diagram also includes an impedance curve, that has been calculated from a simulation, where the hybrid pump model was modelled only with an impedance tube (standard 'Norton, model).

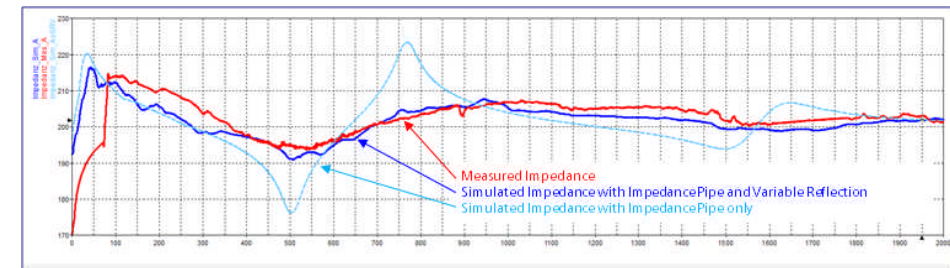


Figure 14: Comparison of measured and simulated pump impedance

From *Figure 14* it is obvious that the amplitude of the impedance calculated from the simulation results of the hybrid pump model matches quite well the impedance of the real 10-chamber vane pump. Compared to the impedance of the standard 'Norton' model, the additional variable impedance is able to smooth the unwanted but unavoidable impedance resonance of the standard 'Norton' model at higher frequencies.

## 6 Summary and Conclusion

The paper presents, at the example of an automotive power steering vane pump, the methodical work steps necessary to create the hybrid pump model. The model has been parameterised merely by means of test rig measurements of the real pump. No additional manufacturer specific information was required.

The validation of the model was made through a simulation of a run-up of the pump, coupled into a simulation model. The direct comparison of amplitude and frequency distribution of pressure pulsations in measurement and simulation data at different pump operating points gave a first proof of the validity of the model and underlined that the hybrid pump model is able to apply realistic flow pulsation onto a 1D system simulation model. Moreover the simulation of 2p/2s-measurements and the comparison of those results with the measured pump showed good correlation and proved that the hybrid pump model is also able to represent the dynamic interaction of a real pump onto the connected hydraulic circuit.

The new hybrid pump model provides a suitable modelling approach, to quickly include the dynamic behaviour of an existing pump into a time-domain based system simulation. Consequently the model will be a valuable remedy whenever the adaptation of the hydraulic ducting to a given pump is focus of the design work.

The authors thank all team members who have contributed to this project, namely Maria Chmielarz, Patrick Leder, Jens Robrecht and Dirk de Ben.

## Nomenclature

Variable	Description	Unit
$A_{RP}$	Cross section of reference pipe and of discharge passageway pipe	[m <sup>2</sup> ]
$B$	Dynamic pressure fluctuation of reflected wave	[Pa]
$c_0$	Speed of sound in fluid	[m/s]
$f_i$	Frequency of pump impedance	[Hz]
$L$	Length of reference pipe in the RaLa test rig	[m]
$l_1, l_2$	Length of additional pipes for 2p/2s system 1 resp. 2	[m]
$l_{RP}$	Length of discharge passageway pipe model	[m]
$p_1, p_2$	Dynamic pressure fluctuations at 2p/2s sensors 1 and 2	[Pa]
$P_1, P_2$	Dynamic pressure fluctuation spectra at sensors 1 and 2 for system 1	[Pa]
$P'_1, P'_2$	Dynamic pressure fluctuation spectra at sensors 1 and 2 for system 2 (')	[Pa]
$p_{S^*}$	Pressure fluctuation at pump flange (without system's feedback)	[Pa]
$p_L$	Pressure fluctuation at pump flange (with system's feedback)	[Pa]
$Q_{S^*}$	Flow fluctuation at pump flange (without system's feedback)	[m <sup>3</sup> /s]
$R_s$	Pump reflection coefficient	[-]
$Z_1, Z_2, Z_R$	Impedances for modelling orifice type resistance	[Pa s/m]
$Z_c$	Impedance of reference pipe	[Pa s/m]
$Z_s$	Pump impedance	[Pa s/m]
$\beta$	Wave propagation coefficient of reference pipe	[1/m]
$\rho$	Density of fluid	[m <sup>3</sup> /kg]

## References

- [1] P. Leder, "Experimental investigations on the hydraulic pump impedance," in XXIII. Deutsch - Polnisches wissenschaftliches Seminar, FH Köln, 2011.
- [2] L. Ericson, On Fluid Power Pump and Motor Design - Tools for Noise Reduction, Linköping University, Ed. Linköping: Linköping Studies in Science and Technology, 2011, vol. Dissertations No. 1417.
- [3] M. Deeken, "Displacement unit simulation in DSHplus," O+P "Ölhydraulik und Pneumatik", vol. 45, no. 2, pp. S. 108-113, 2001.
- [4] E. Goenechea, "Simulationsmodell einer sauggedrosselten Radialkolbenpumpe - Ein Hilfsmittel zur Analyse und Bekämpfung von Flüssigkeitsschall," O+P "Ölhydraulik und Pneumatik", vol. 50, no. 6, pp. 316-321, 2006.
- [5] E. Kojima, "A New Method for the Experimental Determination of Pump Fluid-Borne Noise Characteristics," in Fifth Bath International Fluid Power Workshop, Bath, UK, 1993, pp. 111-137.
- [6] I. Stulemeijer, Beschreibung der Druckschwankungen in hydrostatischen Anlagen und ihre Auswirkungen auf den Luftschall. Eindhoven: Dissertation der Technische Hochschule Eindhoven, 1981.

- [7] K. Wacker, Flüssigkeitsschall in ölhydraulischen Leitungssystemen, Institut für Werkzeugmaschinen der Universität Stuttgart, Ed. Stuttgart: Dissertation der Universität Stuttgart, 1986.
- [8] D. N. Johnston and J.E. Drew, "Measurement of positive displacement pump flow ripple and impedance," IMechE, vol. Part I: Journal of Systems and Control Engineering, pp. 65-74, 1996.
- [9] A. L. Dickinson, "Effects of Discharge Geometry on Hydraulic Power Steering Pump Impedance," in Proceedings for the Dedicated Conference on Mechatronics - Efficient Computer Support for Engineering, Manufacturing, Testing & Reliability, Stuttgart, 1995, pp. 543 - 548.
- [10] J. Liu and D. W. Herrin, "Measuring Acoustic Source Impedance Using Wave Decomposition," in Proceedings of the IMAC-XXVII, Orlando, Florida, USA, 2009.
- [11] K. Habr, Gekoppelte Simulation hydraulischer Gesamtsysteme unter Einbeziehung von CFD, Dissertation Universität Darmstadt, Ed. Darmstadt: Fachbereich Maschinenbau an der Universität Darmstadt, 2002.
- [12] B. Müller, Einsatz der Simulation zur Pulsations- und Geräuschminderung hydraulischer Anlagen. Aachen: Dissertation der RWTH, 2002.
- [13] H. Theissen, Die Berücksichtigung instationärer Rohrströmung bei der Simulation hydraulischer Anlagen, Institut für fluidtechnische Antriebe und Steuerungen, Ed. Aachen: Dissertation der RWTH Aachen, 1983.
- [14] J. Rothmund, Ermittlung von Kennwerten zur Beurteilung der Schallabstrahlung von hydraulischen Systemen, Institut für Werkzeugmaschinen der Universität Stuttgart, Ed. Stuttgart: MVK Medien Verlag Köhler, 1997.
- [15] S. Schellinger and E. Goenechea, "Automated self-regulating system for a low reflection line termination (RaLa)," O+P »Ölhydraulik und Pneumatik«, vol. 47, no. 4, pp. 271-275, 2003.
- [16] S. Berger, Vergleich verschiedener Verfahren zur experimentellen Identifikation der Impedanz von Fluidpumpen, Masterarbeit der Fachhochschule Köln, Ed. Köln, 2011.
- [17] n. n., DSHplus Bauteilhandbuch (Hydraulik). Aachen: FLUIDON Gesellschaft für Fluidtechnik mbH, 2001.